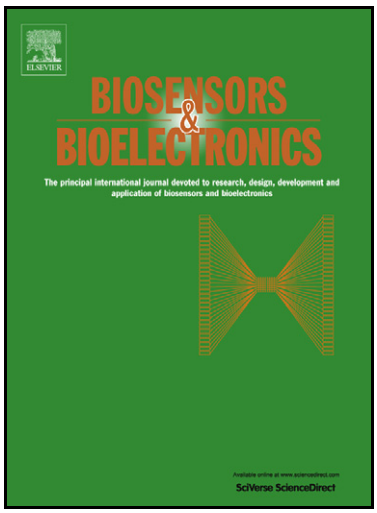

www.elsevier.com/locate/bios

Biomimetic Sensor Based on Hemin/Carbon Nanotubes/Chitosan Modified Microelectrode for Nitric Oxide Measurement in the Brain

Ricardo M. Santos, Marcelo S. Rodrigues, João Laranjinha, Rui M. Barbosa

PII: S0956-5663(13)00017-1
DOI: http://dx.doi.org/10.1016/j.bios.2013.01.015
Reference: BIOS5681

To appear in: *Biosensors and Bioelectronics*

Received date: 16 November 2012
Revised date: 6 January 2013
Accepted date: 7 January 2013

Cite this article as: Ricardo M. Santos, Marcelo S. Rodrigues, João Laranjinha and Rui M. Barbosa, Biomimetic Sensor Based on Hemin/Carbon Nanotubes/Chitosan Modified Microelectrode for Nitric Oxide Measurement in the Brain, *Biosensors and Bioelectronics,* http://dx.doi.org/10.1016/j.bios.2013.01.015

Biomimetic Sensor Based on Hemin/Carbon Nanotubes/Chitosan Modified Microelectrode for Nitric Oxide Measurement in the Brain

Ricardo M. Santos[a], Marcelo S. Rodrigues[a], João Laranjinha[a,b] and Rui M. Barbosa[a,b,*]

[a]*Center for Neuroscience and Cell Biology, University of Coimbra, 3004-517 Coimbra, Portugal*

[b]*Faculty of Pharmacy, University of Coimbra, 3000-548 Coimbra, Portugal*

******Corresponding author: Tel. +351239488463*

Email address: rbarbosa@ff.uc.pt (Rui M. Barbosa).

Abstract

A novel biomimetic microsensor for measuring nitric oxide (NO) in the brain *in vivo* was developed. The sensor consists of hemin and functionalized multi-wall carbon nanotubes covalently attached to chitosan via the carbodiimide crosslinker EDC followed by chitosan electrodeposition on the surface of carbon fiber microelectrodes. Cyclic voltammetry supported direct electron transfer from the Fe^{III}/Fe^{II} couple of hemin to the carbon surface at -0.370 V and -0.305 V vs. Ag/AgCl for cathodic and anodic peaks, respectively. Square wave voltammetry revealed a NO reduction peak at -0.762 V vs. Ag/AgCl that increased linearly with NO concentration between 0.25 and 1 μM. The average sensitivity of the microsensors was 1.72 nA/μM and the limit of detection was 25 nM. Oxygen and hydrogen peroxide reduction peaks were observed at -0.269 V and -0.332 V vs. Ag/AgCl, respectively and no response was observed for other relevant interferents, namely ascorbate, nitrite and dopamine. The microsensor was successfully applied to the measurement of exogenously applied NO in the rat brain *in vivo.*

Keywords:

Nitric oxide microsensor; Hemin; Carbon nanotubes; Chitosan; *In vivo* electrochemistry

Abstract

A novel biomimetic microsensor for measuring nitric oxide (NO) in the brain *in vivo* was developed. The sensor consists of hemin and functionalized multi-wall carbon nanotubes covalently attached to chitosan via the carbodiimide crosslinker EDC followed by chitosan electrodeposition on the surface of carbon fiber microelectrodes. Cyclic voltammetry supported direct electron transfer from the Fe^{III}/Fe^{II} couple of hemin to the carbon surface at -0.370 V and -0.305 V vs. Ag/AgCl for cathodic and anodic peaks, respectively. Square wave voltammetry revealed a NO reduction peak at -0.762 V vs. Ag/AgCl that increased linearly with NO concentration between 0.25 and 1 μM. The average sensitivity of the microsensors was 1.72

nA/μM and the limit of detection was 25 nM. Oxygen and hydrogen peroxide reduction peaks were observed at -0.269 V and -0.332 V vs. Ag/AgCl, respectively and no response was observed for other relevant interferents, namely ascorbate, nitrite and dopamine. The microsensor was successfully applied to the measurement of exogenously applied NO in the rat brain *in vivo.*

Keywords:

Nitric oxide microsensor; Hemin; Carbon nanotubes; Chitosan; *In vivo* electrochemistry

1. Introduction

Nitric oxide (NO) is a key free-radical messenger involved in a wide range of physiological and pathological processes. In the brain, NO can act as a neuromodulator in critical processes including memory. learning and neurovascular coupling (Ledo et al., 2004; Calabrese et al., 2007; Garthwaite, 2008). Given its peculiar physicochemical properties that support a volume signaling process, a detailed knowledge of the cellular actions of NO has been hampered due to difficulties associated with the measurement of its profile of change in biological tissues. Its short half-life and low concentration *in vivo* require the use of sensitive and selective methods possessing high spatio-temporal resolution (Thomas et al., 2008; Santos et al., 2012). Electrochemical methods associated with microelectrodes are particularly attractive for this purpose because of their relative simplicity, good analytical performance and high temporal resolution with minimal damage to tissue (Lama et al., 2012). Various approaches have been made to design NO microsensors with enhanced performance and robustness but the main sensing strategy has been the oxidation of NO at a relatively high potential (+0.9 V), via the utilization of chemically–modified microelectrodes (Bedioui and Villeneuve, 2003; Barbosa et al., 2008; Hetrick and Schoenfisch, 2009; Bedioui et al., 2010). Even so, the selectivity of the NO microsensors is a major concern because many substances present in the brain extracellular space (e.g. ascorbate) are potential interferents when using amperometry.

The electrocatalytic reduction of NO by metalloporphyrins and heme proteins immobilized on electrode surfaces has been less explored but it is an alternative sensing approach taking advantage of the high affinity of NO for transition metals. Hence, there have been numerous reports on the development of NO biosensors based on hemoglobin (Fan et al., 2004), myoglobin (Zhang et al., 2005), Cytochrome C (Koh et al., 2008), horseradish peroxidase (HRP) (Shang et

al., 2004) and microperoxidase (Abdelwahab et al., 2010). Hemin, which has good stability in solution and is relatively inexpensive, has also been used for hydrogen peroxide, oxygen and NO detection (Ye et al., 2004; de Groot et al., 2005; Turdean et al., 2006; Li et al., 2009). The NO biosensors reported so far are based on direct electron transfer (DET) between the immobilized metalloporphyrins or heme-containing proteins and the electrode surface. However, the development of mediator-free, third generation NO biosensors, is however critically dependent on the immobilization procedure of heme proteins due to the deep burying of the heme group in the protein and to the orientation of the protein on the electrode surface (Wu and Hu, 2007).

Carbon nanotubes (CNTs) have been extensively used to enhance electrical contact between heme and the electrode surface due to their unique physical and chemical properties. These materials are usually found in two categories: single wall (SWCNTs) and multiwall (MWCNTs). They provide a high surface-to-volume ratio, promote electron transfer reactions and decrease overpotentials of various electroactive compounds (Agui et al., 2008; Sarma et al., 2009; Vashist et al., 2011). The enhancement of DET of heme proteins by CNTs has been studied by physical adsorption of Hb-MWCNTs on pyrolytic graphite (Zhao et al., 2006) and Mb-MWCNT adsorbed on glassy carbon electrodes (Zhang et al., 2005), by coupling Hb to acid-treated MWCNTs in the presence of EDC (Zhang et al., 2007) or by adsorption of HRP on MWCNTs (Lee et al., 2006). In addition, microperoxidase (MP-11) has been immobilized onto a MWCNT nanocomposite prepared from electrodeposition of gold nanoparticles (AuNPs) and poly-TTCA (Koh et al., 2008).

A critical aspect of the DET and thence of the biosensor performance is the type of immobilization matrix in which CNTs and the biological recognition elements are embedded. A number of biocomposite films have been used, including room temperature ionic liquids (RTILs) (Xu et al., 2010), hydroxylethylcellulose (Liu et al., 2006), carboxymethylcellulose (Huang et al., 2003), cyanoethylcellulose (Jia et al., 2009), layer-by-layer self-assembled film of hyaluronic acid (Barsan et al., 2010) and chitosan (Huang et al., 2002).

Chitosan (Chit) is a linear ß-1,4-polysaccharide obtained by partial deacetylation of chitin from crustaceans that has been used for the immobilization of different enzymes and other biomolecules such as glucose oxidase, glutamate oxidase, lactate oxidase, HRP, tyrosinase and Cyt C (Krajewska, 2004). It is an attractive biocompatible polymer for fabrication of biosensors due to its high mechanical strength, excellent film forming ability and good adhesion, thus

providing a good matrix for immobilization of macromolecules (Krajewska, 2004; Yi et al., 2005). In addition, the presence of reactive primary amines and hydroxyl groups allow advantageous chemical modification of the biopolymer. Because the pKa of Chit ranges from 6.0 to 6.5, its solubility is pH-dependent. Given that in acidic medium most of its primary amines are protonated, Chit exists as a water-soluble cationic polyelectrolyte, but whereas when these groups deprotonate at pH above the pKa the polymer becomes insoluble (Yi et al., 2005).

One of the most commonly methods for Chit film preparation is via cross-linking enzymes using glutaraldehyde or 1-[3-(Dimethylamino)propyl]-3-ethylcarbodiimide (EDC) to form enzyme-Chit gels (Ghica et al., 2009). Electrochemical deposition of Chit onto electrode surfaces was also reported and a series of biosensors have been developed based on this procedure (Krajewska, 2004). The electrodeposition of Chit, particularly by the procedure based on the electroreduction of *p*-benzoquinone as a "proton-consumer" to induce pH-dependent Chit deposition is a very attractive procedure for the immobilization of biomacromolecules on carbon fiber microelectrodes and microelectrode arrays under mild conditions, avoiding loss of biomolecules activity (Zhou et al., 2007).

Noteworthy, most of the NO biosensors described in the literature were evaluated in buffer solutions in the absence of oxygen. This is a serious limitation owing to the potential interference of oxygen which is reduced at a negative potential. Actually, the presence of oxygen in biological media makes the NO measurement based on its electrocatalytic reduction a challenging task.

In the present work, a biomimetic microsensor was designed for the NO measurement in the brain tissue in the presence of oxygen. The electrodeposition of Chit, cross-linked with MWCNTs and hemin by EDC, resulted in microsensors that were able to clearly resolve NO and oxygen reduction peaks, having good electrochemical stability in the presence of physiological brain oxygen concentrations. By using square wave voltammetry, we were able to measure exogenously applied NO *in vivo* in the rat brain.

2. Materials and methods

2.1. Chemicals and solutions

All chemicals were of analytical grade and were used as received. Hemin (>90% from bovine), dopamine (DA), nitrite, ascorbate (AA), dibasic sodium phosphate, monobasic sodium phosphate and sodium chloride and urethane were obtained from Sigma-Aldrich. Hydrogen peroxide (30%) and 3,4-dihydroxyphenylacetic acid (DOPAC) were purchased from Fluka. Chitosan (low molecular weight), *p*-benzoquinone, N-hidroxysuccinimide (NHS) and 1-[3-(Dimethylamino)propyl]-3-ethylcarbodiimide methiodide (EDC) were from Aldrich. Multiwall carbon nanotubes functionalized with carboxyl groups (PD15L1-5-COOH) were obtained from Nanolabs (USA). The solutions were prepared in ultra-pure deionized water (≥18MΩ.cm) from a Milli-Q water purification system, (Millipore Company, Bedford, MA). Phosphate-buffered saline (PBS lite), 0.05 M, pH 7.4 contained: 0.04 M Na_2HPO_4, 0.01 M NaH_2PO_4 and 0.1 M NaCl. NO standard solutions were prepared as previously described (Barbosa et al., 2008; Barbosa et al., 2011)..

2.2. Preparation of the hemin-based microsensors

The carbon fiber microelectrodes (CFMs) were fabricated as previously described (Santos et al., 2008). Three procedures were used for microsensor preparation:

(i) Hemin and MWCNTs adsorption on the CFM surface (sensors referred as CFM/Hemin/MWCNT). A dispersion of MWCNTs in water was prepared by addition of 1 mg of MWCNTs powder to 1 mL of ultra-pure deionized water followed by ultra-sonication during 15 min. The CFMs were first coated with MWCNTs by a dipping procedure, dried for 1 h at room temperature and then dipped for 20 min in 0.3 mM Hemin dissolved in 20 mM NaOH.

(ii) Co-electrodeposition of hemin and MWCNTs with chitosan (sensors referred as CFM/Hemin/MWCNT/Chit). Chitosan at 1% (w/v) was solubilized in 0.9% NaCl under constant stirring during a few hours at pH 4-5. The final pH was set to 5-5.6 by addition of NaOH. A suspension of 1 mg/mL MWCNTs and 20 mg/mL hemin was prepared by addition of MWCNTs and hemin powder to a 20 mM NaOH aqueous solution followed by 10 min ultra-sonication. The final solution used for electrodeposition of chitosan was prepared by mixing 40 μL of 1% Chit

with 40 µL of the MWCNT/hemin suspension followed by addition of 1 mg of *p*-benzoquinone. The CFM tip was immersed in 50 µL of the electrodeposition solution and benzoquinone was reduced by applying a constant potential of -0.5 V vs. Ag/AgCl during 300 s. The reduction of *p*-benzoquinone consumes protons and thereby locally increases the pH at the microelectrode surface, allowing Chit insolubilization (Zhou et al., 2007).

(iii) Hemin and MWCNTs were cross-linked with chitosan using EDC (sensors referred as CFM/Hemin/MWCNT/Chit-EDC). A suspension of 50 µL of MWCNTs/hemin was mixed with 266 µL of 1% Chit and ultrasonicated during 15 min. Then, 121 µL aqueous solution of NHS (50 mg/mL) were added to the mixture and finally 63 µL aqueous solution of EDC methiodide (10 mg/mL) were added under stirring, which was maintained for 1h. Before electrodeposition, 1 mg of *p*-benzoquinone was added to 80 µL of Chit cross-linked with MWCNTs/hemin. The electrodeposition procedure was the same as described in protocol (ii). The microsensors were used at least one day after preparation. Control microsensors based on the three protocols described above but without MWCNTs in the coatings were also prepared.

2.3. Electrochemical measurements

Cyclic Voltammetry (CV) and Square Wave Voltammetry (SWV) experiments were performed using a PGSTAT12 (Ecochemie) running GPES software and IVIUM Compactstat running Iviumsoft. All *in vitro* measurements were performed using an electrochemical cell with three electrode configuration, with the microsensor as working electrode, a platinum wire as auxiliary and an Ag/AgCl (3M KCl) reference. Calibrations in the absence of oxygen were performed in a sealed chamber after bubbling ultrapure argon during 30 min. SWV parameters: f =25 Hz, Es=5 mV, Esw =25 mV. *In vivo* recordings were performed in two electrode configuration mode.

2.4. In vivo experiments

All animal procedures were approved by the local institutional animal care and use committee and were in accordance with the European Community Council Directive for the Care and Use of Laboratory Animals (86/609/ECC). *In vivo* studies were carried out in 8-9 week old wistar rats (260-340 g), as previously described (Barbosa et al., 2008). Briefly, rats were anesthetized with urethane (1.25-1.50 g/kg, i.p.) and placed in a stereotaxic frame (Stoelting Co, USA). A Dremel®

rotary was used to drill a hole in the skull over the brain area of interest. An Ag/AgCl reference electrode (200 μm diameter), prepared from a silver wire, was inserted into the brain through a small hole remote from the recording area. For the preparation of microelectrode/micropipette arrays, a micropipette puller (Sutter Instrument Co, CA) was used to pull glass capillaries (0.58 mm i.d x 1.0 mm o.d.; AM, Systems Inc. WA). The micropipette was attached with its tip positioned at 250 μm from the microelectrode tip using sticky wax and was then filled with a saturated nitric oxide solution in PBS before insertion of the array in the brain. *In vivo* experiments were carried out in the hippocampal CA1 sub-region by using SWV. Small volumes of NO solution (nL range) were pressure ejected from the micropipette using a Picospritzer III (Parker Hannifin Corp., USA).

2.5. Data analysis

Data was analyzed by GPES software and Microcal Origin Pro 7.5. The limit of detection (L.O.D.) was defined as the concentration that corresponds to signal-to-noise ratio of 3. Statistical analysis was performed using GraphPad Prism 5.0. Data is plotted as mean ± S.E.M. and presented in text and tables as mean ± standard deviation (S.D.). The values of *n* represent the number of microsensors used. Differences between two data sets were evaluated by a Student's *t*-test. Statistical tests between multiple data sets were carried out using one- or two-way analysis of variance (ANOVA).

3. Results and Discussion

3.1. Morphology of the composite films

Figure 1 illustrates SEM images of dry hemin/MWCNT composite films prepared by adsorption (A), co-electrodeposition with chitosan (B) and electrodeposition of chitosan cross-linked with hemin/MWCNT (C). Very small differences are evident between SEM images of the surface of the bare carbon fiber (Santos et al., 2008) and the fiber after hemin/MWCNTs coating suggesting that a relatively uniform and thin film of hemin/MWCNTs was formed (Fig. 1A). A film with a rough morphology was observed on the tip of the CFM/Hemin/MWCNT/Chit microsensors (Fig. 1B) due to the electrodeposition of the chitosan/MWCNT/hemin matrix. It is expectable that pH-dependent chitosan precipitation creates a much stronger driving force for co-

deposition of hemin and MWCNTs than simple adsorption upon dipping, because the later relies on relatively weak intermolecular interactions. Accordingly, this rationale might explain the greater accumulation of material on the surface of the fibers induced by Chit/MWCNTs/Hemin electrodeposition than by MWCNTs/Hemin adsorption. A much thicker film appeared on the microsensor surface when MWCNTs and hemin were covalently bound to chitosan (CFM/Hemin/MCWNT/Chit-EDC), as shown in Fig. 1C. Several factors might contribute to the distinct morphology of these coatings: 1) The crosslinking likely forms linkages composed of hemin molecules or MWCNTs that connect adjacent chitosan polymer chains turning the matrix more robust and less porous; 2) The functionalization of the amine groups of Chit can alter its pH-dependent behaviour (e.g. pKa) affecting the electrodeposition process at the microelectrode surface..

3.2. Electrochemical characterization of the hemin-based microsensors

The electrochemical characterization of the three types of composite films was performed by CV to investigate the DET of hemin immobilized on the CFM surface. The enhancement of DET by MWCNTs was also evaluated by comparison with control microsensors that lack MWCNTs in the coatings. Fig. 2A shows voltammograms of a CFM/Hemin/MWCNT/Chit-EDC microsensor recorded at potential sweep rates ranging from 5 to 100 V/s in PBS purged with ultra-pure argon. At a scan rate of 10 V/s, cathodic (Epc) and anodic (Epa) peaks attributed to the Fe^{III}/Fe^{II} couple of hemin were observed at -0.370 ± 0.012 V and -0.305 ± 0.019 V (n=5), respectively, corresponding to a formal potential ($E^{o'}$) of -0.338 V vs. Ag/AgCl. The peak potentials of the Fe^{III}/Fe^{II} couple are in agreement with previous reports supporting DET from hemin (de Groot et al., 2005; Turdean et al., 2006; Li et al., 2009). The corresponding calibration plot of peak current vs. scan rate (ν) from 10 to 100 V/s is depicted in Fig. 2B. The slope of the straight line of Ipc vs. ν is 5.5 nA V^{-1} s (R^2=0.992) and for Ipa is 4.8 nA V^{-1} s (R^2=0.995). The linear relationships are characteristic of a surface-confined electrochemical process. The peak separation of the redox couple at 10 V/s (ΔEp) was 0.065 ± 0.026 V and increased with scan rate, a behaviour that is typical of a quasi-reversible heterogeneous electron transfer process. For scan rates below 5 V/s, the Fe^{III}/Fe^{II} redox couple was not clearly visible on the CVs which might be explained by the geometry and ultra-small size of the microsensors. Average peak potentials of

the Fe^{III}/Fe^{II} couple at a scan rate of 20V/s and the corresponding slopes of peak current vs. scan rate are summarized in Table 1.

An important observation is that the group of microsensors with MWCNTs shows significantly higher slopes of both Ipc and Ipa vs. scan rate than the control group (i.e. sensors without MWCNTs), as assessed by two-way ANOVA (row factor, $p<0.01$). These results confirm the ability of MWCNTs to enhance DET from hemin as expected from their nano-sized structural properties and high electrical conductivity (Cai and Chen, 2004; Agui et al., 2008).

The surface coverage of hemin onto the CFMs was estimated from the CVs based on the equation 1:

$$Ip = \frac{n^2 F^2 \nu \Gamma A}{4 R T} \qquad (1)$$

where n represents the number of electrons transferred, Γ the amount of electroactive hemin adsorbed on the microelectrode, A the tip surface area of microelectrode and ν the scan rate. Considering the geometric area of a cylinder with 250 µm length and 30 µm diameter as representative of the microelectrode shape and the number of electrons transferred n = 1, the calculated amount of hemin immobilized on the CFM surface was 1.7 ± 0.9 x 10^{-11} mol/cm^2 (n=11) for CFM/Hemin/MWCNT/Chit-EDC sensors, 0.98 ± 0.5 x 10^{-11} mol/cm^2 (n=10) for CFM/Hemin/MWCNT/Chit sensors and 2.0 ± 1.7 x 10^{-11} mol/cm^2 (n=7) for CFM/Hemin/MWCNT sensors. The differences between the three types of microsensor were not statistically significant ($p>0.05$, ANOVA), but the values are close to the theoretical coverage calculated for a hemin monolayer of 7 x 10^{-11} mol/cm^2 (Kolpin and Swofford, 1978), suggesting that electroactive hemin forms a monolayer on the microelectrode surface. Thus, the hemin loading into the chitosan matrix with EDC was apparently larger than that obtained by adsorption (or in the absence of EDC) but only a small fraction was effectively electroactive. This is likely due to the non-conducing behaviour of Chit which hampers DET from hemin molecules that are not in close proximity to the microelectrode surface.

The heterogeneous electron transfer rate constant k_s was estimated using the procedure described by Laviron, 1979, when $\Delta Ep < 200/n$ mV, based on the equation 2:

$$m = \frac{RT}{F}\frac{k_s}{nv} \qquad (2)$$

where *m* was graphically related to the separation between anodic and cathodic peaks based on the series of values published by Laviron, 1979, assuming a charge transfer coefficient (α) of 0.5. The estimated k_s was 837 ± 401 s^{-1} (n=9) for CFM/Hemin/MWCNT/Chit-EDC microsensors, 980 ± 346 s^{-1} (n=8) for CFM/Hemin/MWCNT/Chit sensors and 510 ± 343 s^{-1} (n=8) for CFM/Hemin/MWCNT microsensors. No significant differences were found between the three types of microsensors ($p>0.05$, ANOVA). Moreover, the high charge transfer rate constants are in agreement with previous reports for hemin monolayers on the electrode surface, ranging from 160 to 4900 s^{-1} (Sagara et al., 1993; Feng et al., 1995), and are at least two orders of magnitude higher than values obtained for thicker films (Ye et al., 2004; Cao et al., 2012).

3.3. Electrocatalytic reduction of nitric oxide

The electrochemical response of the microsensors to NO was evaluated by SWV following successive additions of a saturated NO solution to PBS in the absence of oxygen. Fig 3 shows a peak at -0.302 V recorded before NO addition using a CFM/Hemin/MWCNT/Chit-EDC sensor which is attributed to the Fe^{III}/Fe^{II} redox couple. Following NO addition, a cathodic peak was observed at -0.763 V due to the electrocatalytic NO reduction by hemin. This value is close to that observed for hemin (de Groot et al., 2005; Li et al., 2009), Hb (Jia et al., 2009) and Mb (Huang et al., 2003).

The electrocatalytic reduction of NO by hemin can be described by the following reaction mechanism (de Groot et al., 2005):

$$\text{Fe(II)} + \text{NO} \longrightarrow \text{Fe(II)-NO}$$

$$\text{Fe(II)-NO} + \text{H}^+ + \text{e-} \longrightarrow \text{Fe(II)-HNO}$$

$$\text{Fe(II)–HNO} + 2\text{H}^+ + 2\text{e-} \longrightarrow \text{Fe(II)} + \text{H}_2\text{NOH}$$

The peak current increased linearly with the NO concentration, from 250 to 1000 nM. The calculated sensitivity was 1.7 ± 0.67 nA/μM and the microsensor's LOD was 25 ± 14 nM (n=16). Comparison with control microsensors showed a slight but significant increase in sensitivity induced by MWCNTs, which is in accordance with the enhancement of DET (Fig. S1). Furthermore, the sensitivity of CFM/Hemin/MWCNT/Chit and CFM/Hemin/MWCNT microsensors was at least 2-fold higher than that of CFM/Hemin/MWCNT/Chit-EDC, which translated into a lower LOD, as summarized in Table 2.

This result could be explained by the much ticker morphology of the Hemin/MWCNT/Chit-EDC composite film, which likely limits the diffusion of NO to the CFM surface, the place where most of the hemin molecules are located. A similar effect exerted by film thickness on the catalytic efficiency was shown to occur in Mb-CMC and Hb-CMC films (Huang et al. 2003). Nevertheless, the sensitivities reported here are much higher than the previously obtained value of 0.34 nA/μM for the same carbon fibers used to measure NO by direct oxidation at +0.9 V (Santos et al., 2008). Furthermore, the LODs in Table 2 are in the range reported for NO detection by direct oxidation using chemically-modified microelectrodes (Bedioui and Villeneuve, 2003; Hrbac et al., 2007; Santos et al., 2008; Brown et al., 2009; Bedioui et al., 2010) which are significantly lower than the LOD of 200 nM reported for the electrocatalytic NO reduction with a carbon-powder microsensor based on hemoglobin (Guo et al., 2008).

A major concern regarding the application of the microsensors for *in vivo* measurements of NO in biological media is the interference of oxygen, which is reduced at negative potentials (Zheng et al., 2002; Ye et al., 2004). Therefore, the electrochemical reduction of oxygen was investigated by adding aliquots of a PBS solution containing 250 μM oxygen to deoxygenated buffer. A cathodic peak which was proportional to oxygen concentration was observed at -0.269 ± 0.033 V (n=8), as shown in Fig. S2A.

The sensitivities of the CFM/Hemin/MWCNT/Chit and CFM/Hemin/MWCNT microsensors were significantly higher than microsensors containing hemin covalently bound to chitosan ($p<0.05$ and $p<0.01$ respectively, table S1). However, the CFM/Hemin/MWCNT/Chit and CFM/Hemin/MWCNT sensors underwent a loss of response in the presence of oxygen. After 100 scans performed in the presence of 40 μM oxygen, the cathodic peak height decreased significantly (Fig. S2C), which contrasts with the oxygen peak stability obtained with the CFM/Hemin/MWCNT/Chit-EDC microsensors (Fig. S2B). Fig. 4A shows that the oxygen peak of CFM/Hemin/MWCNT/Chit-EDC microsensors does not change significantly after 100 consecutive SWV scans, whereas large decreases were found for the other types of sensor. When the oxygen peak was completely lost after successive SWV scans in the presence of oxygen, the microsensors no longer displayed the typical Fe^{III}/Fe^{II} redox couple, nor any electrocatalytic effect towards NO reduction. These results demonstrate that the microsensors containing MWCNTs and hemin covalently bound to chitosan are the most appropriate for NO measurement in biological tissues due to their ability to preserve the electrochemical response of

hemin under physiological oxygen concentrations. The actual mechanism underlying the loss of response that we observed following successive scans in the presence of oxygen has not been elucidated but is probably related with leaching of hemin from the electrode surface. It has been reported that most electrocatalytic systems of metalloporphyrins and substituted phthalocyanine are not very stable due to the porphyrin leaching from the electrode surface (Zheng et al. 2002; Cao et al. 2012). Therefore, a plausible explanation for the CFM/Hemin/MWCNT/Chit-EDC stability is that the covalent binding of hemin to chitosan by EDC stabilizes the microsensor response in the presence of oxygen by preventing the loss of entrapped hemin to the PBS solution.

The response of microsensors to NO was also evaluated in the presence of oxygen (43 µM). Fig. 4B shows typical voltammograms of a CFM/Hemin/MWCNT/Chit-EDC sensor following NO additions in the range of 250-1000 nM. On average, the cathodic peak resulting from electrocatalytic NO reduction appeared at -0.719 ± 0.011 V (n=15), which was significantly lower than in the absence of oxygen (-0.762 ± 0.010 V, $p<0.0001$). Similar peak potentials were obtained for CFM/Hemin/MWCNT/Chit sensors. On contrast, no peaks were recorded with the CFM/Hemin/MWCNT sensors due to the poor electrochemical stability of adsorbed hemin in the presence of oxygen. The average sensitivity of CFM/Hemin/MWCNT/Chit-EDC sensors was 2.6 ± 1.7 nA/µM (n=15) and the L.O.D. was 26 ± 16 nM (n=15). The results are summarized in Table 2.

3.4. Selectivity

The selectivity of the CFM/Hemin/MWCNT/Chit-EDC microsensor against potential interferents present in the brain extracellular space was evaluated. The microsensor did not respond to ascorbate (250 µM), dopamine (8 µM), DOPAC (80 µM) or nitrite (80 µM), as shown in Fig S3A). A catalytic reduction peak at -0.332 V was observed following addition of 20 µM hydrogen peroxide which, however, does not interfere with NO detection in view of the good separation between peaks (Fig. S3B). Overall, these results indicate that the microsensors display a very high selectivity towards NO measurement at its electrocatalytic peak potential, exceeding that of microsensors based on NO oxidation (Bedioui and Villeneuve, 2003; Bedioui et al., 2010). The use of SWV having the advantage of scan speed and high sensitivity over other

electrochemical techniques in association with these microsensors, also offers the chemical resolution that is needed for electrochemical signal identification.

3.5. Nitric oxide measurement in vivo in the rat brain

To establish the proof of concept for the utilization of the CFM/Hemin/MWCNT/Chit-EDC microsensor to measure NO *in vivo* in the rat brain and simultaneously avoid the inherent difficulties associated with the pathways for endogenous NO production, exogenously applied NO was measured *in vivo* in the rat brain. A saturated solution of NO was locally applied at very low volumes (nanoliter range) with the help of a micropipette positioned at 250 μm away from the microsensor tip. Because exogenous NO signals are very short in duration (Santos et al., 2011a; Santos et al., 2011b) high temporal resolution is needed to follow NO concentration changes. Therefore, the potential window used for SWV recordings *in vivo* was shortened to the interval from -0.5 to -1.0 V, corresponding to a scan duration of 2.2 s. Fig. 5A shows a set of scans obtained following local application of 62 nL of NO solution in the rat hippocampus. The maximum peak height was attained at the second scan after NO application, followed by a rapid decrease in the following scans. Typically, NO was detected during the first 4-6 scans after having been ejected from the micropipette. The short duration of the signals (ca. 10 s) is in accordance with previous works using microelectrodes coated with Nafion and *o*-phenylenediamine (Santos et al., 2011b). The peak potential and short signal duration are highlighted in the color plot shown in Fig. 5B. Based on the calibration performed in the presence of oxygen before the experiment, the NO signal in the color plot corresponds to a NO concentration of 1 μM. The NO peak potential measured *in vivo* was -0.850 V which corresponds to a 0.1 V shift as compared with the *in vitro* calibrations. This difference might be related with the composition of the brain extracellular space and the use of a pseudo-reference Ag/AgCl electrode in two electrode configuration mode *in vivo*.

4. Conclusion

The insertion of electrochemical NO microsensors in the brain tissue has been a promising strategy to reveal the profile of NO change but still requiring improvements, particularly in terms of selectivity. The novel microsensor here described takes advantage of the EDC-dependent covalent attachment of hemin and MWCNTs in a biocompatible polymer, chitosan, originating a stable and robust microsensor for brain insertion in the presence of physiological oxygen concentration. Electrochemical characterization by cyclic voltammetry and square wave voltammetry support an excellent electrocatalytic activity for NO reduction in addition to a high sensitivity and a limit of detection in the low nanomolar range. Furthermore, because most compounds present in the brain extracellular space cannot be electrochemically reduced, the microsensor selectivity surpasses that of chemically-modified microsensors based on NO oxidation. Accordingly, no response was observed for several compounds present in the brain extracellular space, including ascorbate, dopamine and nitrite. The biomimetic microsensors were successfully implanted into the rat hippocampus *in vivo* allowing the measurement of exogenous NO applied locally. Nevertheless, the electrocatalytic reduction of oxygen and hydrogen peroxide limits the usefulness of the microsensonsor in the amperometry mode at high negative potentials, which could provide higher temporal resolution. Monitoring the NO produced endogenously *in vivo* in the brain by taking advantage of its electrocatalytic reduction on heme-based microsensors will be the ultimate goal of this work.

Acknowledgements

Financial support from Fundação para a Ciência e Tecnologia (FCT) Portugal, Grant PTDC/SAU-BEB/103228/2008.

RS acknowledges postdoctoral fellowship SFRH/BPD/82220/2011 from FCT.

The authors wish to thank Prof. Christopher Brett, University of Coimbra for reading the manuscript and for helpful discussions.

References

Abdelwahab, A. A., Koh, W. C. A., Noh, H. B., and Shim, Y. B., 2010. Biosens. Bioelectron. *26*, 1080-1086.

Agui, L., Yanez-Sedeno, P., and Pingarron, J. M., 2008. Anal. Chim. Acta *622*, 11-47.

Barbosa, R. M., Lopes Jesus, A. J., Santos, R. M., Lourenco, C. F., Pereira, C. L., Marques, C. F., Rocha, B. S., Ferreira, N. R., Ledo, A., and Laranjinha, J., 2011. Global J. Anal. Chem. *2*, 272-284.

Barbosa, R. M., Lourenco, C. F., Santos, R. M., Pomerleau, F., Huettl, P., Gerhardt, G. A., and Laranjinha, J., 2008. Method. Enzymol. *441*, 351-367.

Barsan, M. M., Pinto, E. M., and Brett, C. M. A., 2010. Electrochimi. Acta *55*, 6358-6366.

Bedioui, F., Quinton, D., Griveau, S., and Nyokong, T., 2010. Phys. Chem. Chem. Phys. *12*, 9976-9988.

Bedioui, F., and Villeneuve, N., 2003. Electroanalysis *15*, 5-18.

Brown, F. O., Finnerty, N. J., and Lowry, J. P., 2009. Analyst *134*, 2012-2020.

Cai, C., and Chen, J., 2004. Anal. Biochem. *325*, 285-292.

Calabrese, V., Mancuso, C., Calvani, M., Rizzarelli, E., Butterfield, D. A., and Stella, A. M. G., 2007. Nature Reviews Neuroscience *8*, 766-775.

Cao, H. M., Sun, X. M., Zhang, Y., Hu, C. Y., and Jia, N. Q., 2012. Analytical Methods *4*, 2412-2416.

de Groot, M. T., Merkx, M., Wonders, A. H., and Koper, M. T., 2005. J. Am. Chem. Soc. *127*, 7579-7586.

Fan, C. H., Liu, X. J., Pang, J. T., Li, G. X., and Scheer, H., 2004. Anal. Chim. Acta *523*, 225-228.

Feng, Z. Q., Sagara, T., and Niki, K., 1995. Anal. Chem. *67*, 3564-3570.

Garthwaite, J., 2008. Eur. J. Neurosci. *27*, 2783-2802.

Ghica, M. E., Pauliukaite, R., Fatibello, O., and Brett, C. M. A., 2009. Sensor Actuat. B-Chem. *142*, 308-315.

Guo, Z. M., Chen, J., Liu, H., and Cha, C. S., 2008. Anal. Chim. Acta *607*, 30-36.

Hetrick, E. M., and Schoenfisch, M. H., 2009. Ann. Rev. Anal. Chem. *2*, 409-433.

Hrbac, J., Gregor, C., Machova, M., Kralova, J., Bystron, T., Ciz, M., and Lojek, A., 2007. Bioelectrochemistry *71*, 46-53.

Huang, H., He, P. L., Hu, N. F., and Zeng, Y. H., 2003. Bioelectrochemistry *61*, 29-38.

Huang, H., Hu, N. F., Zeng, Y. H., and Zhou, G., 2002. Anal. Biochem. *308*, 141-151.

Jia, S. S., Fei, J. J., Zhou, J. P., Chen, X. M., and Meng, J. Q., 2009. Biosens. Bioelectron. *24*, 3049-3054.

Koh, W. C. A., Rahman, M. A., Choe, E. S., Lee, D. K., and Shim, Y. B., 2008. Biosens. Bioelectron. *23*, 1374-1381.

Kolpin, C. F., and Swofford, H. S., 1978. Analytical Chemistry *50*, 916-920.

Krajewska, B., 2004. Enzyme Microb. Tech. *35*, 126-139.

Lama, R. D., Charlson, K., Anantharam, A., and Hashemi, P., 2012. Anal. Chem. *84*, 8096-8101.

Laviron, E., 1979. J. Electroanal. Chem. *101*, 19-28.

Ledo, A., Frade, J., Barbosa, R. M., and Laranjinha, J., 2004. Mol. Aspects Med. *25*, 75-89.

Lee, Y. M., Kwon, O. Y., Yoon, Y. J., and Ryu, K., 2006. Biotechnol. Lett. *28*, 39-43.

Li, C. Z., Alwarappan, S., Zhang, W., Scafa, N., and Zhang, X., 2009. Am. J. Biomed. Sci. *1*, 274-282.

Liu, X. J., Chen, T., Liu, L. F., and Li, G. X., 2006. Sensor Actuat. B-Chem. *113*, 106-111.

Sagara, T., Takagi, S., and Niki, K., 1993. J. Electroanal. Chem. *349*, 159-171.

Santos, R. M., Lourenco, C. F., Gerhardt, G. A., Cadenas, E., Laranjinha, J., and Barbosa, R. M., 2011a. Neurochem. Int. *59*, 90-96.

Santos, R. M., Lourenco, C. F., Ledo, A., Barbosa, R. M., and Laranjinha, J., 2012. Int. J. Cell Biol. *2012*, 391914.

Santos, R. M., Lourenco, C. F., Piedade, A. P., Andrews, R., Pomerleau, F., Huettl, P., Gerhardt, G. A., Laranjinha, J., and Barbosa, R. M., 2008. Biosens. Bioelectron. *24*, 704-709.

Santos, R. M., Lourenco, C. F., Pomerleau, F., Huettl, P., Gerhardt, G. A., Laranjinha, J., and Barbosa, R. M., 2011b. Antioxid. Redox Sign. *14*, 1011-1021.

Sarma, A. K., Vatsyayan, P., Goswami, P., and Minteer, S. D., 2009. Biosens. Bioelectron. *24*, 2313-2322.

Shang, L. B., Liu, X. J., Fan, C. H., and Li, G. X., 2004. Annali di Chimi. *94*, 457-462.

Thomas, D. D., Ridnour, L. A., Isenberg, J. S., Flores-Santana, W., Switzer, C. H., Donzelli, S., Hussain, P., Vecoli, C., Paolocci, N., Ambs, S., Colton, C. A., Harris, C. C., Roberts, D. D., and Wink, D. A., 2008. Free Radical Biol. Med. *45*, 18-31.

Turdean, G. L., Popescu, I. C., Curulli, A., and Palleschi, G., 2006. Electrochim. Acta *51*, 6435-6441.

Vashist, S. K., Zheng, D., Al-Rubeaan, K., Luong, J. H. T., and Sheu, F. S., 2011. Biotechnol. Adv. *29*, 169-188.

Wu, Y. H., and Hu, S. S., 2007. Microchim. Acta *159*, 1-17.

Xu, Y. X., Hu, C. G., and Hu, S. S., 2010. Anal. Chim. Acta *663*, 19-26.

Ye, J. S., Wen, Y., De Zhang, W., Cui, H. F., Gan, L. M., Xu, G. Q., and Sheu, F. S., 2004. J. Electroanal. Chem. *562*, 241-246.

Yi, H. M., Wu, L. Q., Bentley, W. E., Ghodssi, R., Rubloff, G. W., Culver, J. N., and Payne, G. F., 2005. Biomacromolecules *6*, 2881-2894.

Zhang, L., Zhao, G. C., Wei, X. W., and Yang, Z. S., 2005. Electroanal. *17*, 630-634.

Zhang, R., Wang, X., and Shiu, K. K., 2007. J. Colloid Interf. Sci. *316*, 517-522.

Zhao, L., Liu, H., and Hu, N., 2006. J. Colloid Interf. Sci. *296*, 204-211.

Zheng, N., Zeng, Y., Osborne, P. G., Li, Y., Chang, W., and Wang, Z., 2002. J. Appl. Electrochem. *32*, 129-133.

Zhou, Q. M., Xie, Q. J., Fu, Y. C., Su, Z. H., Jia, X., and Yao, S. Z., 2007. J. Phys. Chem. B *111*, 11276-11284.

Figure legends

Fig. 1. SEM images of the surface of hemin-based microsensors. Typical SEM images with same magnification (5000x) of (A) hemin/MWCNT (B) hemin/MWCNT/Chit and (C) hemin/MWCNT/Chit-EDC composite films.

Fig. 2. Characterization of hemin electrochemical behavior by cyclic voltammetry. (A) Cyclic voltammograms of a CFM/Hemin/MWCNT/Chit-EDC microsensor, potential sweep rate range from 5 to 100 V/s. (B) Plot of peak current vs. scan rate, slopes 5.5 nA V^{-1} s for the cathodic peak (R^2=0.992) and 4.8 nA V^{-1} s for the anodic peak (R^2=0.995).

Fig. 3. Microsensor response to nitric oxide in the absence of oxygen. (A) Square wave voltamograms recorded with a CFM/Hemin/MWCNT/Chit-EDC microsensor following successive NO additions corresponding to final concentrations of 250, 500 and 1000 nM. A cathodic peak appeared at -0.763 V. The peak height was proportional to NO concentration with a sensitivity of 1.6 nA/µM (R^2=0.978). SWV parameters: *f* =25 Hz, *Es*=5 mV, *Esw* =25 mV.

Fig. 4. Microsensor stability and response to nitric oxide in the presence of oxygen. (A) Average oxygen reduction peak height recorded by SWV (relative to the first scan) for the three types of microsensor after 30, 60 and 100 scans in the presence of 43 µM of oxygen. *, $p<0.05$; **, $p<0.01$; ***, $p<0.001$ vs. peak height of the first scan (n=4-8). (B) Square wave voltammograms recorded with a CFM/Hemin/MWCNT/Chit-EDC microsensor following successive NO additions corresponding to final concentrations of 250, 500 and 1000 nM in the presence of 43 µM oxygen. A cathodic peak appeared at -0.717 V. The peak height was proportional to NO concentration with a sensitivity of 6.5 nA/µM (R^2=0.927).

Fig. 5. Exogenous nitric oxide measurement in the brain *in vivo.* Nitric oxide was measured upon pressure ejection of a saturated nitric oxide solution from a micropipette at 250 µm distance from the CFM/Hemin/MWCNT/Chit-EDC microsensor in the rat hippocampus. (A) Representative baseline-subtracted square wave voltammograms, following pressure ejection of 62 nL of NO solution. (B) Corresponding color plot of current intensity illustrating the voltammograms.

Fig S1. Effect of carbon nanotubes on nitric oxide sensitivity. The bars show average sensitivities of the three kinds of microsensors fabricated (legend) with and without MWCNTs (control). The *p* values indicated were calculated by using two-way ANOVA to assess the effect of MWCNTs on the microsensors response. The results are plotted as mean ± S.E.M..

Fig. S2. Response of microsensors to oxygen. Oxygen reduction by the microsensors was evaluated by addition of oxygen from a PBS solution (250 µM) to the supporting electrolyte, previously bubbled with argon. (A) SWV (baseline-subtracted) obtained with a CFM/Hemin/MWCNT/Chit-EDC microsensor following successive additions of oxygen corresponding to final concentrations of 12, 23, 32 and 43 µM, (captions *a* to *d)*. A cathodic peak was observed at -0.25 V that was proportional to the oxygen concentration (see inset). The slope of the trend line was 0.24 nA/µM (R^2=0.998). Cathodic oxygen peaks in the presence of 43 µM of oxygen, recorded after 30, 60 and 100 scans are shown for a CFM/Hemin/MWCNT/Chit-EDC (B) and a CFM/Hemin/MWCNT/Chit microsensor (C).

Fig. S3. Evaluation of microsensor selectivity. (A) super-imposed SWV scans obtained with a CFM/Hemin/MWCNT/Chit-EDC microsensor in PBS in the absence of oxygen for 1 µM NO, 80 µM NO_2^-, 250 µM ascorbate (AA), 8 µM dopamine (DA) and 80 µM 3,4-dihydroxyphenylacetic acid (DOPAC). (B) SWV scans in PBS containing 20 µM hydrogen peroxide (red trace), which was followed by addition of 1 µM NO. The cathodic peaks for H_2O_2 and NO reduction were observed at -0.332 V and -0.737 V, respectively.

Table 1-Electrochemical characterization of direct electron transfer of Fe^{III}/Fe^{II} in immobilized hemin

Microsensor	**Epc (V)**	**Epa (V)**	**Slope Ipc vs. scan rate (nA V^{-1} s)**	**Slope Ipa vs. scan rate (nA V^{-1} s)**
CFM/Hemin	-0.373 ± 0.012 (3.2%) (n=4)	-0.297 ± 0.048 (16%) (n=4)	-1.15 ± 0.41 (36%) (n=4)	0.81 ± 0.36 (44%) (n=4)
CFM/Hemin/MWCNT	-0.396 ± 0.031 (7.6%) (n=8)	-0.281 ± 0.023 (8.1%) (n=8)	-4.59 ± 3.67 (80%) (n=7)	3.72 ± 3.12 (84%) (n=3)
CFM/Hemin/Chit	-0.436 ± 0.022 (5.0%) (n=6)	-0.287 ± 0.086 (30%) (n=6)	-1.40 ± 0.80 (57%) (n=9)	0.87 ± 0.31 (36%) (n=9)
CFM/Hemin/MWCNT/Chit	-0.389 ± 0.018 (4.6%) (n=11)	-0.319 ± 0.024 (7.5%) (n=11)	-2.22 ± 1.18 (53%) (n=10)	1.59 ± 1.02 (64%) (n=10)
CFM/Hemin/Chit-EDC	-0.377 ± 0.017 (4.5%) (n=5)	-0.289 ± 0.029 (10%) (n=5)	-2.45 ± 0.59 (24%) (n=5)	2.09 ± 0.63 (30%) (n=5)
CFM/Hemin/MWCNT/Chit-EDC	-0.382 ± 0.018 (4.7%) (n=13)	-0.286 ± 0.021 (7.4%) (n=13)	-3.82 ± 1.95 (51%) (n=11)	3.08 ±1.51 (49%) (n=11)

The data are given as the mean ± SD (CV).

The number of microelectrodes tested is given in parenthesis.

Table 2- Microsensor electrochemical response to NO

	Absence of oxygen			Presence of oxygen (43 µM)		
Microsensor	**NO peak (V)**	**Sensitivity (nA/µM)**	**LOD (nM)**	**NO peak (V)**	**Sensitivity (nA/µM)**	**LOD (nM)**
CFM/Hemin/MWCNT	-0.737 ± 0.004 (0.6%) (n=8)	4.62 ± 1.66 (36%)* (n=7)	7.9 ± 3.87 (49%)* (n=7)	-	-	-
CFM/Hemin/MWCNT/Chit	-0.752 ± 0.009 (1.2%) (n=12)	4.19 ± 1.55 (37%)* (n=12)	12.2 ± (9.15) 75% (n=12)	-0.705 ± 0.015 (2.1%)[#] (n=7)	4.29 ± 3.52 (82%) (n=5)	13 ± 3.8 (29%) (n=5)
CFM/Hemin/MWCNT/Chit-EDC	-0.762 ± 0.011 (1.4%) (n=17)	1.72 ± 0.67 (39%) (n=16)	25 ± 15 (58%) (n=16)	-0.719 ± 0.012 (1.6%)[#] (n=15)	2.61 ± 1.67 (64%) (n=15)	26 ± 15 (59%) (n=15)

The data are given as the mean ± SD (CV).

The number of microelectrodes tested is given in parenthesis.

*, $p<0.05$ vs. CFM/Hemin/MWCNT/Chit-EDC; [#], $p<0.0001$ vs. in the absence of oxygen.

Highlights

- A microsensor for nitric oxide (NO) is designed based on a novel nanocomposite film.
- Cyclic voltammetry shows direct electron transfer from hemin.
- The electrocatalytic reduction of NO provides high sensitivity and selectivity.
- The microsensor is able to resolve NO and oxygen peaks by square wave voltammmetry.
- Measurement of exogenously applied NO *in vivo* in the rat brain is demonstrated.

A

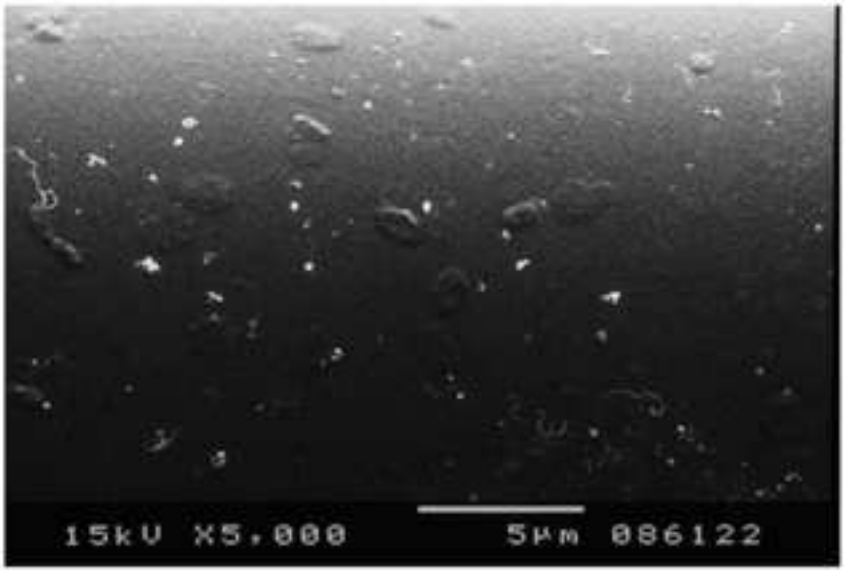

B

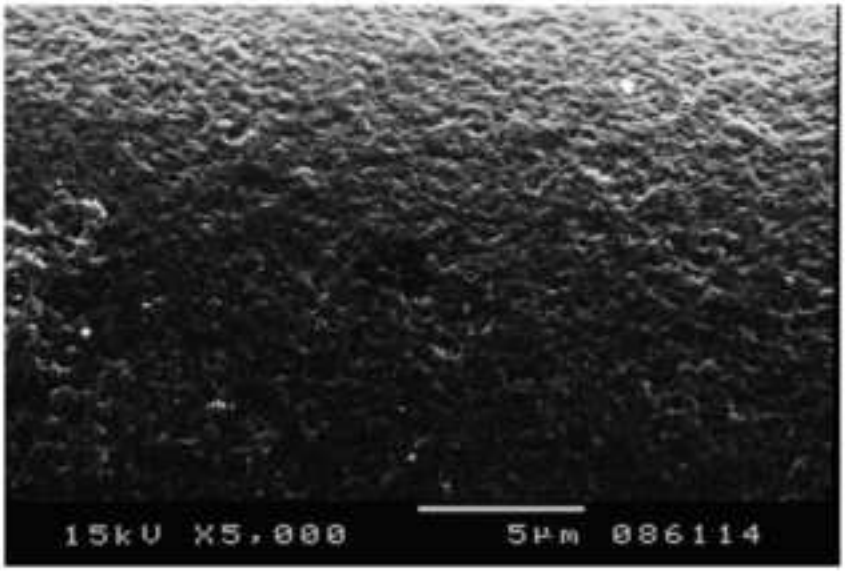

C